

# Effect of gamut expansion of object colours on a simulated six-primary display

Chun-Kai Chang, Yoko Mizokami, Hirohisa Yaguchi, Pei-Li Sun<sup>1</sup> and Hung-Shing Chen<sup>2</sup>

*Graduate School of Advanced Integration Science, Chiba University, Japan*

<sup>1</sup>*Graduate Institute of Color and Illumination Technology, National Taiwan University of Science and Technology, Taiwan*

<sup>2</sup>*Graduate Institute of Electro-Optical Engineering, National Taiwan University of Science and Technology, Taiwan*

*Email: hibadinao520@yahoo.com.tw*

This paper evaluates the gamut expansion ratio on a six-primary display by conducting a psychophysical experiment involving real objects. However, no six-primary display was used in this article; it was based on the simulated and virtual RGBCMY display. We first introduce the algorithm for simulating the six-primary display that consists of three stages: (1) colour separation, (2) code condensation, and (3) white point estimation. To ensure that we identify the most suitable gamut expansion ratio for the human perception of the colours of objects, our experiments featured pineapple, loquat, wax apple, peach, plum, carambola, and guava fruits through saturated colours on a monitor. Subjects were asked to identify their preferences for the colours that they observed. Our results show that the most suitable perception range for real objects is from 1.2 to 1.4.

*Received 15 December 2015; revised 26 January 2017; revised 27 June 2017; accepted 27 June 2017*

*Published online: 02 August 2017*

## Introduction

Recent advancements in display devices have led to the development of wide-gamut devices. These devices typically extend the display colour gamut using two techniques: (1) by improving the purity of RGB primaries, and (2) by adding more colour primaries other than RGB. With the rising popularity of multi-primary technologies, some companies have also launched corresponding display devices and technics [1-3]. Accordingly, this paper also focuses on the multi-primary colour display technique.

Given their wider gamut, multi-primary display devices can reproduce most colours found in nature. Some previous studies have identified the gamut of natural colours. Pointer used four databases containing 36 hue angles and sampled each degree of lightness at 16 levels to define 4,089 colours in the range of natural colours [4]. Moreover, he updated the range of surface colours [5]. In 1999, Tajima *et al.* collected a total of 49,672 natural colours from the natural world and developed them into a standard object colour spectra (SOCS) database [6]. In 2004, Tajima *et al.* compared the SOCS data with the Pointer's surface colour set and identified only small differences between them suggesting that both can serve as reliable gamuts of natural colours [7]. However, Tajima *et al.* also showed that the range of natural colours is wider than that originally defined by Pointer or the SOCS database, thus suggesting that the colour gamut of nature requires further update and refinement [8-9]. Figure 1 shows the gamuts of object colours as defined by Pointer, the SOCS database, the sRGB and the AdobeRGB, which are the largest colour ranges in normal RGB displays. The gamut of the colours of objects in nature is wider than that of these displays.

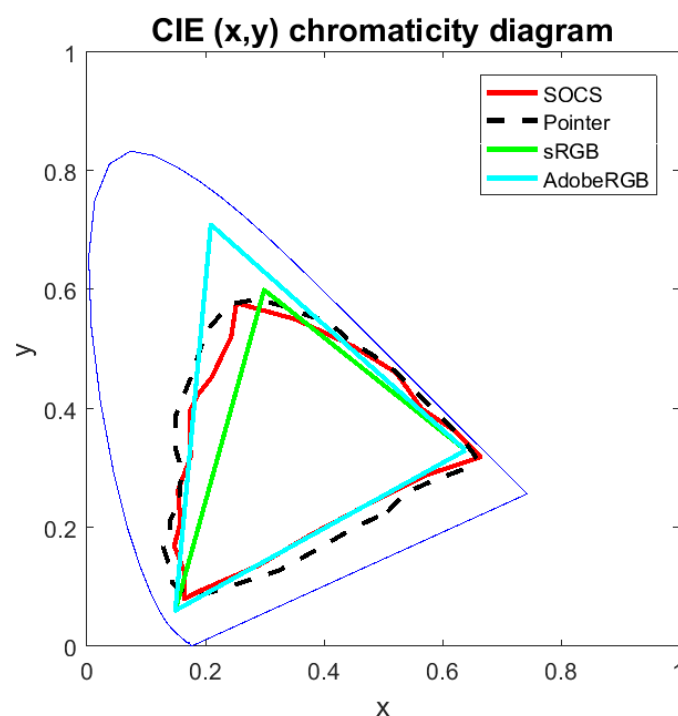


Figure 1: The gamuts of the SOCS database, Pointer's data, the sRGB, and the AdobeRGB colour spaces.

Multi-primary techniques can extend the display gamut further, but this becomes complicated in terms of signal control. Conventional six-primary colour conversion applies various constraints in the transfer of RGB input values to six-primary signals [10-12]. In general, this process enhances the purity of cyan (C), magenta (M), and yellow (Y), but reduces their luminance. This colour mismatch phenomenon was also observed in the early days of cross-media reproduction. Reproducing a colour from one device to another often requires the luminance of the colours to be modified. As an example, converting a larger colour gamut to correspond to a smaller colour gamut is a technique known as the gamut reduction algorithm. Research on mathematical calculation methods to this end [13-16] has led to the description of an ideal gamut boundary description, for cross-media reproductions from a colour gamut in a CRT (Cathode ray tube) or LCD (Liquid crystal display) monitor to that in a cyan, magenta, yellow, or key/black printer. This approach yields the best perceptual performance that most closely matches real objects on each device [17].

Gamut mapping techniques have recently been applied to conversion between images and multi-primary displays. Since the colour gamut has increased with the evolution of display devices, research on gamut extension algorithms has also grown; examples here include the gamuts of printers and high-definition television systems [18], the enhancement of whole-colour images, application to film [19-20], and the wide colour gamut specifications of the International Color Consortium profiles, such as sRGB [21] and xvYCC [22].

With regard to the application of gamut mapping techniques, many studies have indicated that gamut mapping that adjusts lightness (i.e., luma) and the chroma in the CIELCh colour space is effective. Furthermore, research has shown that people prefer simultaneous gamut mapping modulation of lightness and chroma with a fixed hue [23-26].

In our six-primary system described here, we chose a combination of normal RGB and CMY primary colours [27]. The conventional colour reproduction architecture of CMY is based on the Neugebauer model [28], which shows that the given reflectance consists of an overprint of the primary colours and secondary colours as well as a three-colour overprint. Our six-primary system is also inspired by this model, simultaneously simulating six primaries on a display device. Therefore, Neugebauer's colour separation method is an important issue here. We also use the under colour removal (UCR) and grey component replacement (GCR) methods in our six-primary algorithm. The combined UCR/GCR method solves the problem of superimposition in halftone screens by determining the amount of black to display from the specific amounts of CMY colours. Given that the characteristics of the display comprise the colours obtained from the additive colour mixing method, we determine the amount of white as a parameter by adding these three channels. By using this parameter, we can simulate the CMY channel that is would be added to the display.

In this study, we aim to find a suitable colour boundary of real object colours in a six-primary display. Although our multi-primary display system is close to the preferences identified in human perception, we had general images such as portraits and outdoor scenery for its assessment. Hence, we had not confirmed whether the same enhancement ratio for colour expansion is pertinent to natural objects with saturated colours.

Given the above, we evaluate object colour preference for a six-primary display simulated in a conventional RGB display because there is no physical six-primary display with RGB and CMY colours combined. We used images of real fruits as stimuli to obtain a suitable enhancement ratio for the colour reproduction of natural objects, as fruits are suitably representative of the colours of objects in nature.

## Method

### *Colour primaries*

We constructed a hypothetical six-primary system based on data describing RGB LED lamps. We measured the spectral distribution of the RGB LEDs (Stanley Electric) by using a Konica Minolta CS-1000A spectroradiometer, and calculated the CIE1931 (x,y) chromaticity coordinates of the RGB primaries. Complementary colours were set at the intersection point of the line starting from one primary colour through the D65 white point to that connecting the other two primary colours. The expansion ratios of the original complementary colours to the newly defined primaries of cyan, magenta and yellow colours were 1.4, 1.2, and 1.1, respectively. Figure 2 shows the scheme plot of complementary and primary colours.

Following the above, we optimised the RGB/CMY luminance ratio based on Yang *et al.*'s principle [29]. The white point we defined was D65, but the luminance ratios of RGB and CMY were set to 1:1.5 to avoid losing the luminance balance in our six-primary system.

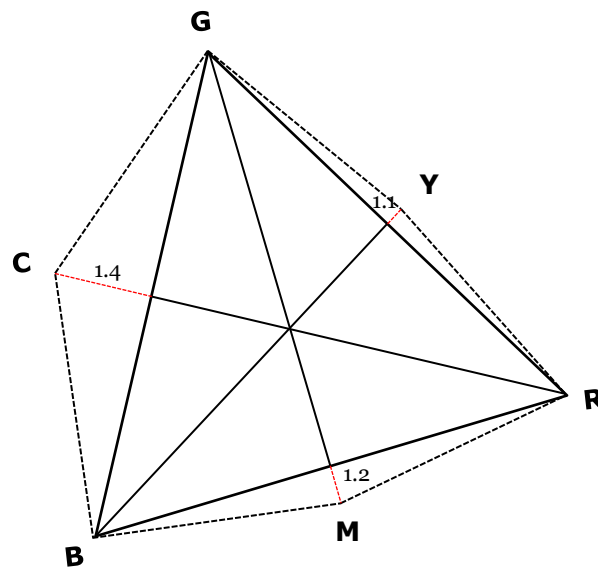


Figure 2: The relationships between complementary and primary colours with their expansion ratios.

### Colour separation

Our colour separation method that we use is based on the UCR/GCR method described above. We derive a brightness-adjustable RGB-to-RGB/CMY colour separation model to generate RGB-to-RGB/CMY data for different brightness levels,  $p$ , ranging from 0.0 to 1.0 at intervals of 0.1. Our model is described as follows: Figure 3 shows the flowchart design of our six-primary algorithm.



Figure 3: Colours separation flowchart.

In the RGB sorting step, we sort the RGB values and obtained the maximum, middle, and minimum values of  $R$ ,  $G$ , and  $B$ . These correspond to  $H$ ,  $E$ , and  $L$ , respectively, in Equation 1.

$$\begin{cases} H = \max(R, G, B) \\ E = \text{mid}(R, G, B) \\ L = \min(R, G, B) \end{cases} \quad (1)$$

In the grey extraction step, we define  $L$  as a grey component and  $L_c$  as the complementary colour to  $L$ . In the second primary extraction, we define the CMY values. If  $H$  is equal to  $L$ , the colour is achromatic; otherwise,  $H_c$ ,  $E_c$ , and  $L_c$  the complementary colours of  $H$ ,  $E$ , and  $L$ , respectively can be described using  $L$  and  $L_c$ , as shown in Equation 2. The  $H'$ ,  $E'$ ,  $L'$ , and  $H'_c$ ,  $E'_c$ ,  $L'_c$  represent the new results of the RGB and CMY values, respectively.

$$\text{otherwise} \left\{ \begin{array}{l} L_c = E - L \\ H' = (H - E) + L + p \cdot L_c \\ E' = L + p \cdot L_c \\ L' = L \end{array} \right. \left| \begin{array}{l} \text{if } H = L \text{ then } \begin{cases} H' = E' = L' = L \\ H'_c = E'_c = L'_c = p \cdot L \end{cases} \\ \begin{cases} H'_c = p \cdot L \\ E'_c = p \cdot L + 0.5 \cdot p \cdot (H - E) \\ L'_c = p \cdot L + L_c + 0.5 \cdot p \cdot (H - E) \end{cases} \end{array} \right. \quad (2)$$

$$\text{otherwise} \left\{ \begin{array}{l} L_c = E - L \\ H' = H - (1 - p) \cdot L_c \\ E' = L + p \cdot L_c \\ L' = L \end{array} \right. \left| \begin{array}{l} \text{if } H = L \text{ then } \begin{cases} H' = E' = L' = L \\ H'_c = E'_c = L'_c = p \cdot L \end{cases} \\ \begin{cases} H'_c = p \cdot L \\ E'_c = 0.5 \cdot p \cdot (H + L - L_c) \\ L'_c = E'_c + L_c \end{cases} \end{array} \right. \quad (3)$$

### Code condensation

Although the colour gamut resulting from the above is wide, its brightness is lower than that of a normal RGB system. Therefore, we apply brightness enhancement in the next step, for which we add  $p \times L$  to each of the complementary primaries, where  $p$  is the brightness enhancement factor. The relationship between the RGB/CMY primary colours and the  $p$ -factors is illustrated in Figure 4. When the  $p$ -factor increases, there is an increase in luminance in the CIE 1976  $L^*a^*b^*$  colour space.

The last issue to be resolved is that the addition of cyan, magenta and yellow colours results in a significant chroma reduction. Therefore, we add a step to enhance the dominant colours, where we replace  $L_c$  with  $p \times L_c$  in  $H$  and  $E$  in the parts of the dominant colours; further, we replace  $0.5 \times p \times (H - E)$  in the  $L_c$  and  $E_c$  parts. We can then simplify Equation 2 can then be simplified to yield Equation 3 by substituting  $L_c + L$  for  $E$ :

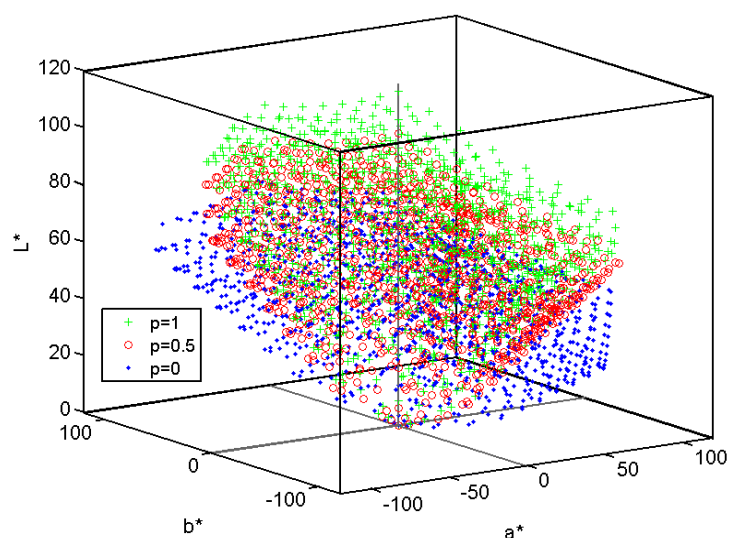


Figure 4: Three-dimensional graph showing the relationship between RGB/CMY primary and  $p$ -factors in the CIE 1976  $L^*a^*b^*$  colour space.

### White point estimate

Finally, as part of our model, we must provide a white point mapping, because the sampled white point is D65, which corresponds to  $(Y, C_b, C_r)=(235, 128, 128)$  in the eight-bit xvYCC colour space [22]. If we map the white point of our  $p = 0$  sub-gamut to the sRGB white, it is much darker than normal RGB displays. On the contrary, if we choose  $p = 1$ , we obtain a substantial mismatch between the six-primary display and the sRGB standard gamut. Through optimisation analysis, we find that  $p = 0.25$  is the most appropriate value here; thus, to ensure the balance, we use a  $p = 0.25$  white point versus the sRGB white. Using this value of  $p$ , the volume of the full 3D six-primary display gamut versus the sRGB white. The volume of the full 3D six-primary display gamut is 168% of that of the sRGB in CIE 1976  $L^*a^*b^*$  colour space.

### Estimating the expansion ratios of complementary colour primaries

We then examine the expansion ratios suitable for natural objects. We attempt to redesign the expansion ratios of the CMY colour primaries. Note that we don't change the expansion ratios of CMY individually, but at the same rates. To simplify the calculation and avoid image colour dependencies, the expansion ratios were modified from 1.0 to 2.0 at intervals of 0.2.

### Optimisation method using the gamut mapping method

While it is well known that clipping or nearest sampling methods are often used, for cross-media reproductions from a larger gamut to a smaller gamut, these methods cause many expanded colours to be mapped to the same colours even though they originally have different brightness and saturation levels. Therefore, we use our own unique gamut mapping method that maintains the relative positional ratio of each colour between the two colour gamuts. Using this approach, we can map the expanded colours onto the AdobeRGB gamut without experiencing any clipping.

Figure 5 shows the scheme of our proposed gamut mapping algorithm. Based on the above, this algorithm was applied to the lightness-chroma plane of the CIELCH colour space. We preserved the  $Y$  (i.e., luma) channel to simulate the  $L$  (i.e., lightness) channel, subtracting 128 from both the  $C_b$ , and the  $C_r$  channels to simulate the  $a^*$ , and  $b^*$  channels, respectively, in the CIE 1976  $L^*a^*b^*$  colour space. The conversion from CIELCH to CIE 1976  $L^*a^*b^*$  is defined as follows.

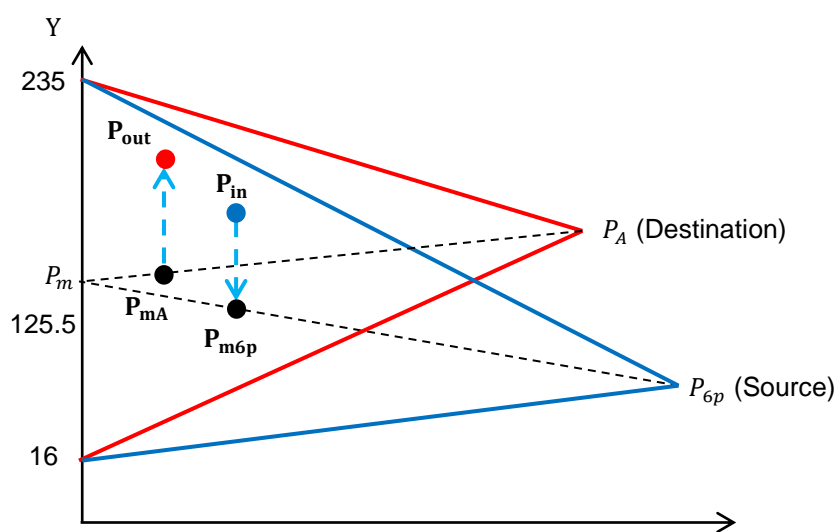


Figure 5: Scheme of the proposed gamut mapping method.

$$\begin{cases} L = Y \\ C = \sqrt{(C_b - 128)^2 + (C_r - 128)^2} \\ H = \tan^{-1}(C_r - 128 / C_b - 128) \end{cases} \quad (4)$$

In Figure 5, the blue and red lines show the calculated colour gamut and the six-primary displays, respectively. In the figure, we define the midpoint of the luminance range as  $P_m$  along the y-axis. Because luminance  $Y$  in the  $YC_bC_r$  colour space ranges from 16 to 235, we identify  $P_m$  as 125.5 (i.e., the midpoint between 16 and 235). Furthermore,  $P_A$  and  $P_{6p}$  denote the most saturated points, i.e., the cusp in a AdobeRGB monitor and the six-primary gamut, respectively.

Any given cusp at any given hue angle can be derived from the nearby primary colour cusps of  $R$ ,  $G$ ,  $B$ ,  $C$ ,  $M$ , or  $Y$ . In Equation 5,  $t$  can be considered an interpolation coefficient derived from the  $C_b$  and  $C_r$  values of the two initial six-primary colours  $(C_{b1}, C_{r1})$  and  $(C_{b2}, C_{r2})$ , respectively.

$$t = \frac{C_{b1} \times \tan(h) - C_{r1}}{(C_{r2} - C_{r1}) - \tan(h) \times (C_{b2} - C_{b1})} \quad (5)$$

The calculation of the cusp value  $YC_bC_r$  can be used by the two initial six-primary colours  $(C_{b1}, C_{r1})$  and  $(C_{b2}, C_{r2})$  as well as  $t$ , which are computed as follows:

$$\begin{cases} Y = Y_1 + (Y_2 - Y_1) \times t \\ C_b = C_{b1} + (C_{b2} - C_{b1}) \times t \\ C_r = C_{r1} + (C_{r2} - C_{r1}) \times t \end{cases} \quad (6)$$

where  $P_{in}$  indicates the arbitrary input colour point from the six-primary gamut; thus, the saturation ratio of to its cusp can be represented as  $C_{ratio} = P_{in} / P_{6p}$ . The shapes of Adobe RGB and the six-primary gamut were sufficiently close enough here. Furthermore, the saturation value of  $P_{out}$  can be represented as  $C_{out} = C_{ratio} \times P_A$ . Also,  $P_{m6p}$  is located on the line connecting  $P_m$  and  $P_{6p}$ ; thus,  $P_{m6p}$  is defined as follows:

$$P_{m6p} = 125.5 + C_{ratio} \times (P_{6p} - 125.5) \quad (7)$$

Similarly, the  $P_{mA}$  can be represented as follows:

$$P_{mA} = 125.5 + C_{ratio} \times (P_A - 125.5) \quad (8)$$

Finally, the output luminance  $Y_{out}$  can be obtained as follows:

$$Y_{out} = P_{mA} + (Y_{mv(6p)} - P_{m6p}) \quad (9)$$

However, this display also considers the characteristics of visual perception in the lightness–chroma plane. Thus, as shown in Figure 6, we divide the entire gamut into four regions, where the centre of these regions has a lightness level of 50% and a chroma level of 50%.

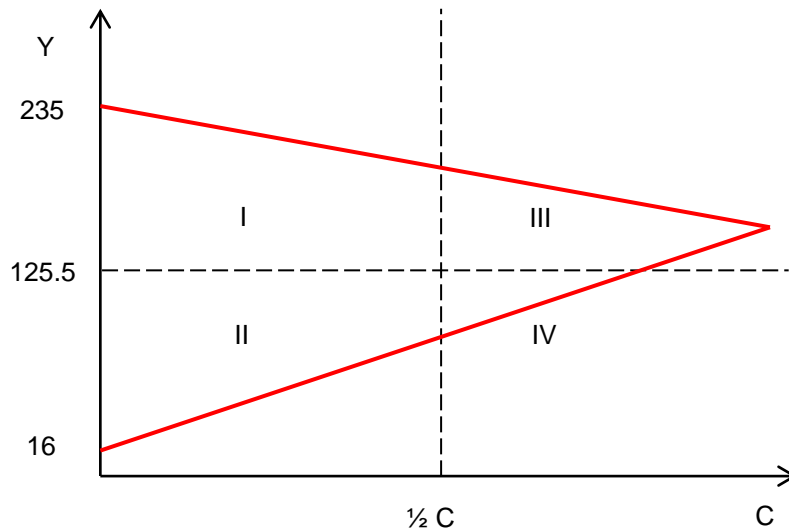


Figure 6: The four regions in the L-C plane.

To determine the parameters of  $Y$  and  $C$ , we conducted a psychophysical experiment to simultaneously adjust values along the  $Y$  (i.e., lightness) and  $C$  (i.e., chroma) axes values in these four regions by judging 10 stimuli and identifying the colours perceived best. According to results of an assessment involving 12 subjects, the average values of the parameters of  $Y$  for each region were 1.01, 0.953, 0.944, and 0.900, while those of parameters of  $C$  for each region were 0.988, 1.021, 1.012, and 0.957.

Given the above, the new output luminance  $Y_{n\_out}$  and output chroma  $C_{n\_out}$  can be written as follows.

$$Y_{n\_out} = Y_I \times Y_{out} + Y_{II} \times Y_{out} + Y_{III} \times Y_{out} + Y_{IV} \times Y_{out} \quad (10)$$

$$C_{n\_out} = C_I \times C_{out} + C_{II} \times C_{out} + C_{III} \times C_{out} + C_{IV} \times C_{out} \quad (11)$$

## Experiment

After transforming the colour stimuli into our six-primary environment, we conducted a psychophysical experiment to determine the relationship between the effects of colour enhancement and human perception. Figure 7 shows a flowchart of our experiments.

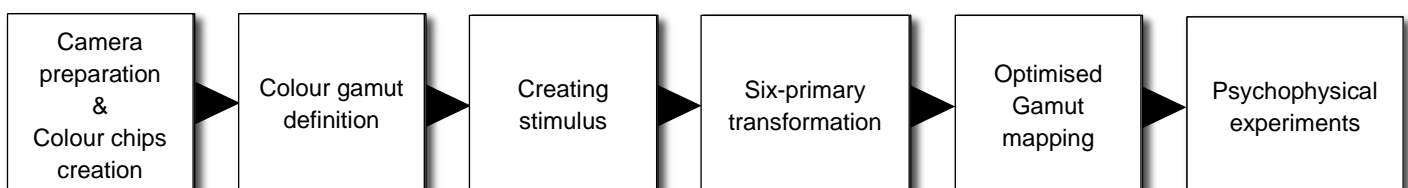


Figure 7: Flowchart showing our psychophysical experiment.

### Experimental device settings

For our visual evaluation experiments, we used an EIZO monitor (CG242W) with the AdobeRGB colour gamut. We calibrated this monitor based on the measurement data from 500 colour patches covering the full ranges of the monitor gamut by using an Eye One spectroradiometer.

We then prepared images captured by three cameras. Our goal was to compare the differences in image characteristics depending on camera type. Cameras 1 and 3 were traditional digital cameras, a Canon S95 and a Sony Cyber-shot DSC-T100, whereas camera 2 was a mirrorless SLR (Sony NEX-7). The white balance of each camera was set manually by focusing on a white patch on the Eizo monitor corresponding to D65 white. To examine the gamut of each camera, we displayed five colour patches – the three primary colours red, green, and blue, and white and black – at the center of the monitor photographed it. The image files (using the RAW format for each image) were then obtained from each camera. Following this, we displayed each image on the same Eizo monitor and measured the CIE(x, y) chromaticity coordinates with a Konica Minolta CS-1000 spectroradiometer. Figure 8 shows the gamut of each camera and the Eizo monitor. The gamut of the colours was smaller than that of AdobeRGB, indicating the limitations of colour reproduction.

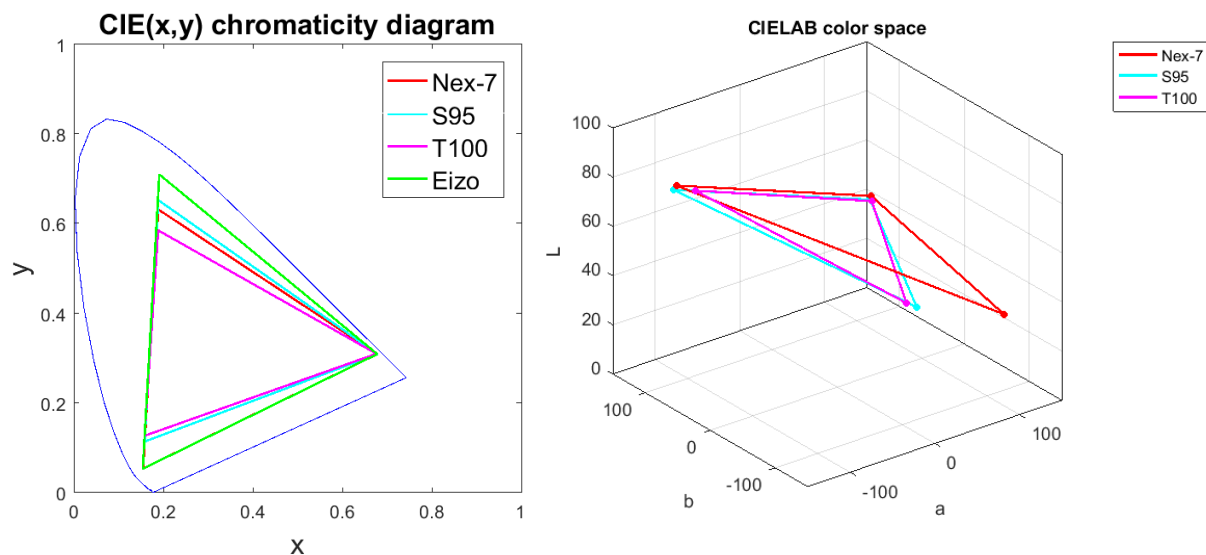


Figure 8: The gamut of each camera and the Eizo monitor in CIE(x,y) chromaticity diagram (left) and CIELAB colour space (right).

### Experimental stimuli

As shown in Figure 9, we used seven fruits with saturated colours as experimental stimuli: pineapple, loquat, wax apple, peach, plum, carambola, and guava. To avoid the influence of background or surrounding colours during the visual experiment, all images were taken in an entirely white environment containing a white plate and a white table. Even though a grey background is often used in visual evaluations, we used white for ours because food and fruits are more commonly placed on white tables.

According to past researches, a suitable appearance of an object usually depends on its colour, shape, and surface [30]; thus, we fixed the latter two variants to determine the colour boundary that the observers could best perceive. All images were taken under the same lighting conditions with a fluorescent lamp that simulated D65 white.



Figure 9: The seven stimuli (first row from left to right: pineapple, loquat, wax apple and peach; second row from left to right: plum, carambola and guava).

We then transformed all images into the six-primary colour space by using the Equation 2. Figure 10 shows an example of the transformation. We adjusted the gamut expansion ratio of yellow, cyan, and magenta simultaneously, preparing images with ratios ranging from 1.2 to 2.0 at intervals of 0.2. The original represents the camera's RAW file. We used six stimulus images for each fruit for a total of 42 total images for each camera.



Figure 10: Stimuli in the original sRGB (i.e., the leftmost) and the expanded six-primary stimuli.

We conducted psychophysical experiments to determine the preferable expansion ratios of our six-primary display. As shown in the schematic Figure 11, the psychophysical experiments were conducted in a dark room containing an Eizo monitor. All subjects sat on a chair and looked directly at the monitor at a distance of 30cm.

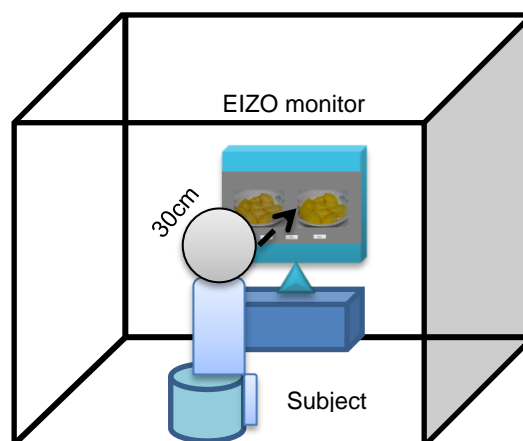


Figure 11: Psychophysical experiment set up.

Figure 12 shows an example of the interface of the monitor. The background colour was set to Munsell colour N7. As shown in the figure, two images were presented side by side. The visual angle of each stimulus was  $32.13^\circ \times 25.36^\circ$ . Furthermore, two “Better” buttons and an “Undo” button were

located at the bottom of the screen. Note that the size of the monitor was 24.1 inches, its resolution was  $1920 \times 1200$ , and the aspect ratio was 16:10.

We used a paired comparison method for evaluation. The subjects were instructed to identify the stimulus that they found most attractive. Note that none of the subjects observed the original stimulus until he/she had conducted the psychophysical experiment. After three minutes of dark adaptation, and one minute of light adaptation, the subjects chose the stimulus they preferred by selecting the “Better” button under the corresponding stimulus. They repeated this procedure for each combination of the expansion ratio, for one image with six ratios, and without repetition, i.e., 15 ( $6 \times 5 / 2$ ) combinations; each pair was presented randomly. If the subjects were unable to make a decision, they were allowed to press the “Undo” button to skip the given pair; however, the skipped combination was presented again later in the experiment; thus, judgments for all combinations were eventually obtained.

When the subjects completed the combinations for a given image, the next set of images was presented to them. They saw the same pairs of images taken by the three cameras in the three separate sessions.

Ten subjects (six male and four female), participated in the experiment, each with normal colour vision and visual acuity, or a corrected visual acuity of approximately 1.0. The ages of the subjects ranged from 22 to 30 years old.

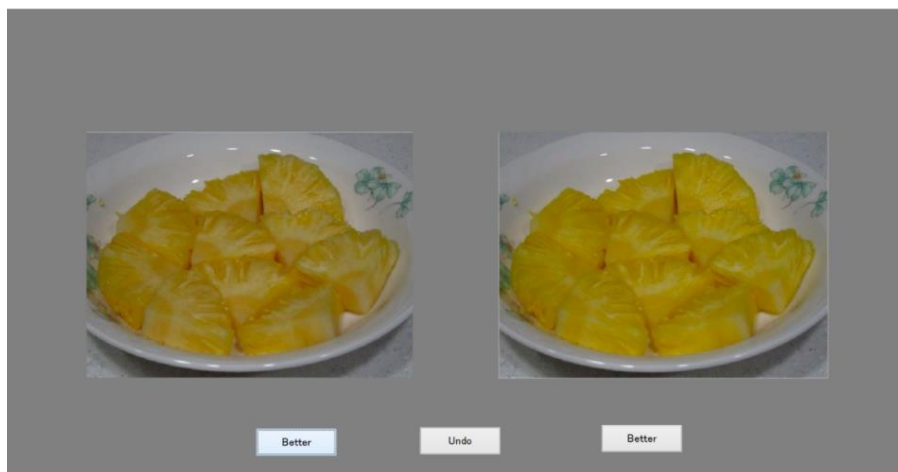


Figure 12: Interface of the psychophysical experiment.

## Results and discussion

The evaluation of our results followed Case 5 of the Law of Comparative Judgment identified by Thurstone [31]. The value of the psychological scale between stimuli A and B was simplified as shown in Equation 12 below. In Case 5, as the correlation of  $\rho_{AB}$  was zero, and that of  $\sqrt{\sigma_A^2 + \sigma_B^2}$  was one, we could only directly refer to the  $Z$  values according to the difference between subjects to evaluate the image quality.

$$S_A - S_B = Z_{A-B} \sqrt{\sigma_A^2 + \sigma_B^2 - 2\rho_{AB} \cdot \sigma_A \sigma_B} \quad (12)$$

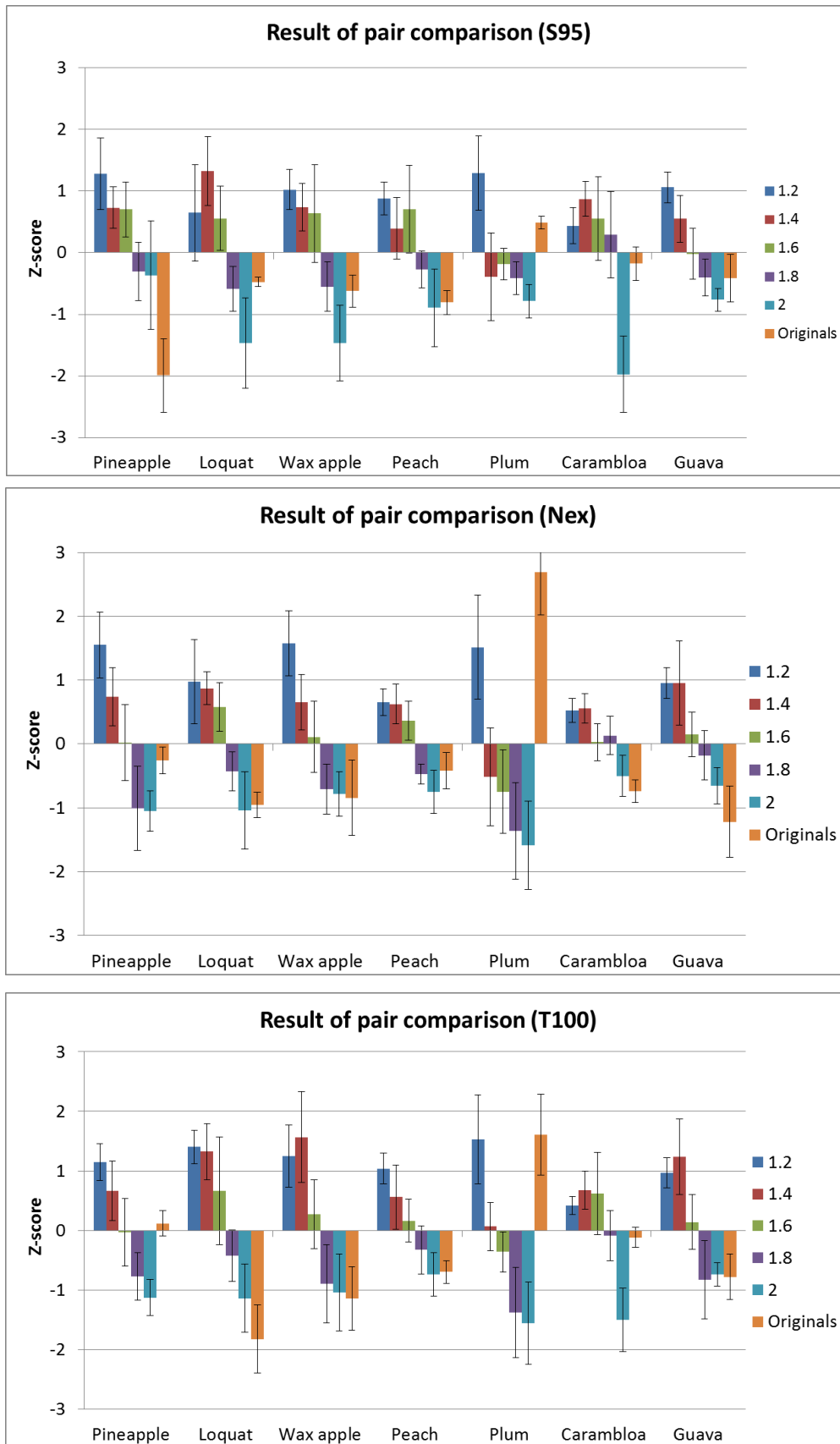


Figure 13: Psychophysical results of each stimulus for the three cameras – S95 (top), Nex (middle), and T100 (bottom).

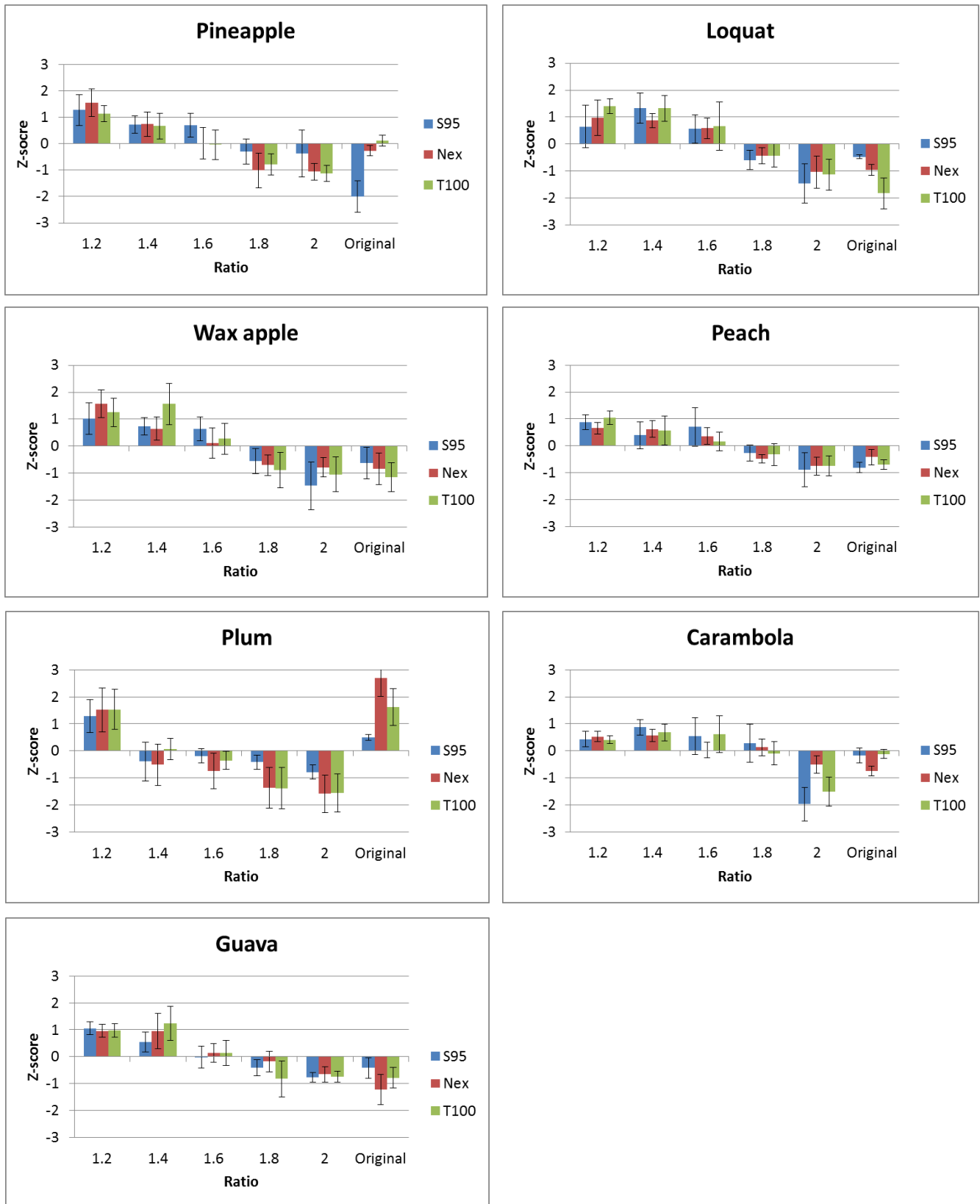


Figure 14: Gamut expansion results of psychophysical experiment.

Figure 13 shows the preferences of all subjects. The ratios here range from 1.2 to 2.0, corresponding to each fruit from left to right, whereas the error bars show the 95% confidence intervals across the population.

Figure 14 shows the preferences of all subjects for each fruit. The vertical axis shows the degree of preference of subjects, represented as a Z-score. The higher the Z-score, the higher the preference for the given fruit. In each plot, as with Figure 14, from left to right, the ratios range from 1.2 to 2.0, with the last set representing the original results. The results correspond to each fruit imaged by each of the three cameras, with S95, Nex, and T100 represented in blue, red, and green colors, respectively. The error bars in each plot for each ratio show 95% confidence intervals of our psychophysical experiments.

### **ANOVA results**

For each camera used for each stimulus, we perform a one-way analysis of variance (ANOVA) to determine if the camera specification influenced the overall results. For each expansion ratio, we calculated an F-value for each of 1.2, 1.4, 1.6, 1.8, and 2.0 as ( $F(2,18) = 0.430$ ,  $p > 0.05$ ), ( $F(2,18) = 0.768$ ,  $p > 0.05$ ), ( $F(2,18) = 1.509$ ,  $p > 0.05$ ), ( $F(2,18) = 1.343$ ,  $p > 0.05$ ), ( $F(2,18) = 0.532$ ,  $p > 0.05$ ), and ( $F(2,18) = 0.154$ ,  $p > 0.05$ ), respectively, and found no statistical differences among the cameras. This clearly showed that if the stimuli were due to differences in colour among cameras in terms of different colour gamuts and sensitivities, this did not seriously affect the results.

For each camera, we then determined if there were significant differences among the expansion ratios. Our results yielded ( $F(5,36) = 17.630$ ,  $p < 0.01$ ), ( $F(5,36) = 8.356$ ,  $p < 0.01$ ), and ( $F(5,36) = 16.196$ ,  $p < 0.01$ ) for the S95, Nex and T100 cameras, respectively. These results indicate that the level of “attractive” changes based on the perception of colour changes in the stimuli produced by all cameras.

### **Post-hoc results**

As all our experiments involved the same subjects and expansion ratios, we used Tukey’s post-hoc test to determine if there were significant differences in a given ratio. For camera S95, the original, 1.8 and 2.0 reached their levels of significance at ratios 1.2 and 1.4 with  $p < 0.05$ ; however, for the Nex camera, there was a significant difference only at ratio 1.2 with  $p < 0.05$ ; similarly, ratios 1.2 and 1.4 in the T100 camera had significant differences with  $p < 0.01$ . By taking the intersection of these three results, we determined that the expansion ratio was approximately situated at 1.2 – 1.4. Significant results in the original also indicated that it is necessary to develop a multi-primary display, because the colour expansion caused subjects to prefer the perceived content.

There were significant differences among all fruits that, however, occurred at different ratios. For the pineapple, with ( $F(5,12) = 8.152$ ,  $p < 0.01$ ), a preference at a ratio of 1.2 was much higher than those at 1.8, 2.0, and the original. For the loquat, there were significant differences between preferences at ratios of 1.2 and 1.4 and those at 1.8, 2.0, and the original; the F value was ( $F(5,12) = 27.492$ ,  $p < 0.01$ ). For the carambola, only 1.4 had significant differences with ratio 2.0 and the original, with ( $F(5,12) = 11.614$ ,  $p < 0.01$ ).

The wax apple, peach, and guava, except at 1.2 and 1.4, had significant differences among one another, and their F values were ( $F(5,12) = 30.166$ ,  $p < 0.01$ ), ( $F(5,12) = 45.658$ ,  $p < 0.01$ ), and ( $F(5,12) = 28.451$ ,  $p < 0.01$ ), respectively. Finally, for the plum, our results stood out in that the original and the ratio 1.2 recorded significant differences in preference with the others, i.e., ( $F(5,12) = 14.444$ ,  $p < 0.01$ ).

Although we found significant differences in many results of the paired comparisons, there were small differences in the optimised ratios among the stimuli. Since yellow was directly affected by the expansion ratios, the subjects were inclined to choose the higher ratio when observing fruits that had them; however, fruits containing some green and red colours were not directly affected by the expansion ratios; here, the subjects hesitated to choose between ratios 1.2 and 1.4. Finally, plum is a dark-blue fruit; thus, the effect of colour expansion was marginal.

In general, the subjects preferred the original or only slightly enhanced stimuli in choosing suitable ratios; we conclude that too much expansion leads to counter-effective results.

From the relationships in each ratio for each fruit, given that they often had no significant differences between ratios 1.2 and 1.4, and given that some objects have low or moderate saturation levels in nature, the suitable ratio for multi-primary expansion is 1.3.

As shown in Figure 15, we can also view this trend for each ratio via a box plot; here, the figure shows the box plot of psychophysical statistical values for each ratio from all stimuli in all cameras. The upper and lower values of each box plot in each ratio were 75% and 25%, while the error bars were at the maximum and minimum psychophysical values from all psychophysical values, respectively.

Palmer *et al.* showed that people prefer objects containing brighter colours to those containing darker ones [32]. Many researchers have also shown that factors such as gender, race, and progressive technologies slightly affect the preferences and memory of the colours of objects [33-35].

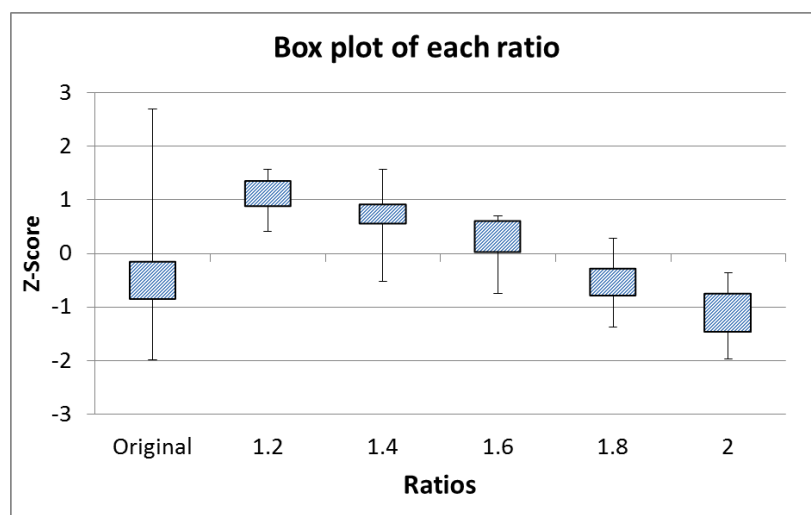


Figure 15: A box plot corresponding to each ratio.

Some studies have shown that when observers watch objects in nature, their preferences and memories of the hue and brightness are at the same levels as the originals; but in saturation, they are prone to a more saturated perception [36-37]. This is also the reason why many manufacturers use a wider gamut of backlight components to replace the traditional display [38-39]. Our findings for the preferences for ratios are consistent with those results.

Even though we used the images of fruits, our results agree with those of past research on preference using various images and objects. This implies that we can apply our findings to other natural objects. However, the subjects in this experiment knew the original fruits, and hence experience and memory might have influenced the results. Further investigation using familiar as well as unfamiliar stimuli is necessary to obtain more generalised suitable expansion ratios.

## Conclusions

In this paper, we proposed a six-primary RGBCMY wide-gamut system developed by ourselves and a CMY colours expansion algorithm based on modified GCR/UCR method by considering the complementary colours expansion algorithm. Using a paired comparison experiment, we determined suitable expansion ratio for fruits to be preferable in terms of vividness and found some significant relationships between colour enhancement and preference in wide-gamut systems. Images taken by all three cameras that we used were equally preferred by the subjects. We found that a suitable ratio for expansion is about 1.3 (Range from 1.2 to 1.4) in general.

## References

1. Choe W, Lee DS and Kim CY (2005), Studying for multi-primary LCD, *Proceedings of the SPIE (Color Imaging X: Processing, Hardcopy, and Applications)*, **5667**, 336-343.
2. Chino E (2006), Development of wide-color-gamut mobile displays with four-primary-color LCDs, *SID Symposium Digest of Technical Papers*, 1223-1224.
3. Teragawa M, Yoshida A, Yoshiyama K, Nakagawa S, Tomizawa K and Yoshida Y (2012), Multi-primary-color displays: The latest technologies and their benefits, *Journal of the Society for Information Display*, **20** (1), 1-11.
4. Pointer MR (1980), The gamut of real surface colors, *Color Research and Application*, **5** (3), 145-155.
5. Pointer MR (2002), Request for real surface colors, *Color Research and Application*, **27** (5), 374.
6. Tajima J, Inui M and Azuma Y (1999), Development of standard object colour spectra database for colour reproduction evaluation (SOCS), *Journal of The Society of Photographic Science and Technology of Japan*, **62** (2), 126-135.
7. Inui M, Hirokawa T, Azuma Y and Tajima J (2004), Color gamut of SOCS and its comparison to Pointer's gamut, *Proceedings of the International Conference on Digital Printing Technologies*, 410-415, Salt Lake City (USA).
8. Li C, Luo MR and Pointer MR (2007), A colour gamut based on reflectance functions, *Proceedings of the Fifteenth Color Imaging Conference*, 213-217, Albuquerque (USA).
9. Perales E, Chorro E, Viqueira V and Martínez-Verdú F (2009), Estimation of the real colour gamut, *Proceedings of the Eleventh Congress of the International Colour Association (AIC Colour 2009)*, 71-76, Sydney (Australia).
10. Ajito T, Ohsawa K, Obi T, Yamaguchi M and Ohyma N (2001), Color conversion method for multiprimary display using matrix switching, *Optical Review*, **8** (3), 191-197.
11. Takaya M, Ito K, Ohashi G and Shimodaira Y (2005), Fast color conversion for multiprimary displays using a classification technique, *Proceedings of the SPIE (Color Imaging X: Processing, Hardcopy, and Applications)*, **5667**, 344-353.
12. Sugiura H, Kaneko H, Kagawa S, Ozawa M, Tanizoe H, Ueno H, Kimura T and Kato H (2005), Wide-color-gamut and high-brightness WUXGA LCD monitor with color calibrator, *Proceedings of the SPIE (Color Imaging X: Processing, Hardcopy, and Applications)*, **5667**, 554-561.
13. Stone MC, Cowan WB and Beatty JC (1998), Color gamut mapping and the printing of digital color images, *ACM Transactions on Graphics*, **7** (4), 249-292.
14. Oittinen P, Autio H and Saarelma H (1992), Color gamut in halftone printing, *Journal of Imaging Science and Technology*, **36** (5), 496-501.
15. Dilawari JS and Khanna R (2012), Reproduction of images by gamut mapping and creation of new test charts in prepress process, *International Journal of Scientific and Engineering Research*, **3** (10).  
<https://www.ijser.org/onlineResearchPaperViewer.aspx?Reproduction-of-Images-by-Gamut-Mapping-and-Creation-of-New-Test-Charts-in-Prepress-Process.pdf>
16. Braun KM, Fairchild MD and Alessi PJ (1996), Viewing techniques for cross-media image comparisons, *Color Research and Application*, **21** (1), 6-17.

17. Morovic J and Luo MR (2001), The fundamentals of gamut mapping: a survey, *Journal of Imaging Science and Technology*, **45** (3), 283-290.
18. Hoshino T (2013), A preferred color reproduction method for the HDTV digital still image system, *Proceedings of the International Conference on Future Information and Communication Engineering*, 559-568, City (Country).
19. Anderson H, Garcia EK and Gupta MR (2007), Gamut expansion for video and image sets, *Proceedings of the Fourteenth International Conference of Image Analysis and Processing Workshops*, 188-191, Modena (Italy).
20. Zamir SW, Vazquez-Corral J and Bertalmío M (2014), Gamut mapping in cinematography through perceptually-based contrast modification, *Proceedings of the IEEE Transactions on Image Processing*, **8** (3), 490-503.
21. IEC 61966-2-2:2003 Multimedia systems and equipment – Colour measurement and management Part 2-2: Colour management–Extended RGB colour space–sRGB.
22. IEC 61966-2-4:2006 Multimedia systems and equipment - Colour measurement and management Part 2-4: Colour management–Extended-gamut YCC colour space for video applications–xvYCC.
23. Montag ED and Fairchild MD (1997), Psychophysical evaluation of gamut mapping techniques using simple rendered images and artificial gamut boundaries, *Proceedings of the IEEE Transactions on Image Processing*, **6** (7), 977-989.
24. Kato N, Ito M and Ohno S (1999), Three-dimensional gamut mapping using various color difference formulae and color space, *Journal of Electronic Imaging*, **8** (4), 365-379.
25. Kang BH, Morovic J, Luo MR and Cho MS (2003), Gamut compression and extension algorithms based on observer experiment data, *Journal of the Electronics and Telecommunications Research Institute (ETRI)*, **25** (3), 156-170.
26. Bonnier N, Schmitt F, Brettel H and Berche S (2006), Evaluations of spatial gamut mapping algorithms, *Proceedings of the Fourteenth Color Imaging Conference*, 56-61, Scottsdale (USA).
27. Sun P-L, Chen H-S and Chang C-K (2008), Six-primary LCD color separation for wide-gamut xyYCC images, *Proceedings of the Fifteenth Display Workshops*, 1425-1428, Niigata (Japan).
28. Neugebauer HEJ (1957), Color correction selector, US Patent No. 2790844 (30 April 1957).
29. Yang Y-C, Song K, Rho S, Rho N-S, Hong S, Deul KB, Hong M, Chung K, Choe WH, Lee S, Kim CY, Lee S-H and Kim H-R (2005), Development of six-primary LCD, SID Symposium Digest of Technical Papers, **36** (1), 1210-1213.
30. Ikeda M and Shidoji K (2006), Relationship between delicious-looking feelings and visual features of cakes, *The Institute of Electronics, Information and Communication Engineers (IEIC) Technical Report*, **106** (410), 51-56.
31. Thurstone LL (1927), A law of comparative judgement, *Psychological Review*, **34**, 278-286.
32. Palmer SE and Schloss KB (2010), An ecological valence theory of human color preference, *Proceedings of the National Academy of Sciences of the United States of America*, **107** (19), 8877-8882.
33. Palmer SE and Schloss KB (2011), Ecological valence and theories of human color preference, in *New Directions in Colour Studies*, Biggam CP, Hough C, Simmons D and Kay C (eds.), 361-376, Amsterdam: John Benjamins.
34. Yoshizawa K, Schloss KB, Asano M and Palmer SE (2015), Ecological effect in cross-cultural differences between US and Japan color preference, *Cognitive Science*, **40** (7), 1590-1616.
35. Smet KAG, Lin Y, Nagy BV, Németh Z, Duque-Chica GL, Quintero JM, Chen H-S, Luo MR, Safi M and Hanselaer P (2014), Cross-cultural variation of memory colors of familiar objects, *Optics Express*, **22** (26), 32308-32328.
36. Siple P and Springer RM (1983), Memory and preference for the colors of objects, *Attention, Perception & Psychophysics*, **34** (4), 363-370.
37. Bartleson CJ (1960), Memory colors of familiar objects, *Journal of the Optical Society of America*, **50** (1), 73-77.
38. Lee MH, Seop SM, Kim JS, Hwang JH, Shin HJ, Cho SK, Min KW, Kwak WK, Jung SI, Kim CS, Choi WS, Kim SC and Yoo EJ (2009), Development of 31-inch full-HD AMOLED TV using LTPS-TFT and RGB FMM, *Journal of Information Display*, **40** (1), 802-804.
39. McRae BM (2013), Using quantum dots for extending the color gamut of LCD displays, US Patent No. 9356204 (05 December 2013).